Vehicles Modeling and Multi-Sensor Smoothing Techniques for Post-Processed Vehicles Localisation

David Bétaille - *Laboratoire Central des Ponts et Chaussées - France*
Philippe Bonnifait - *Heudiasyc UMR 6599 - Université de Technologie de Compiègne - France*

BIOGRAPHY

David Bétaille is a junior researcher at the LCPC (the French public works research institute), and belongs to the Site Robotics subdivision. He has been involved in vehicles location using DGPS and dead-reckoning for several years, supervising last year the development of an industrial prototype based on his design. In the meanwhile, David Bétaille has undertaken a research program at University College London, about multipath in kinematic GPS (a subject closely connected with precise positioning of machines on roadworks), with the aim of completing a PhD in geodesy and navigation.

Philippe Bonnifait is an assistant professor at the Université de Technologie de Compiègne. His research activities concern non linear systems state estimation. The major application considered is the localisation process of vehicles using GPS, dead-reckoning techniques and digital road maps. In 1997, he has participated to the Brite-Euram CIRC project for the development of the localisation module of compactors. He is now with the Heudiasyc UMR 6599 and he works on the evaluation of driving assistance systems in the frame of the 5th PCRD European project "Roadsense".

ABSTRACT

The present paper reports the latest experimental results of a prototype system developed by LCPC with technical assistance of Heudiasyc for its pavement management vehicles. Specification requirements can be summarized by

- one meter precision,
- for regional itineraries,
- including urban environment,
- in a navigation post-processing.

Dedicated geo-synchronous satellites services provide differential GPS corrections suitable for the application concerned. The assistance of dead-reckoning sensors to estimate the position of the vehicle during DGPS masks enables the continuity of localisation.

An improvement of an original algorithm for post-processing the trajectory of the vehicle is presented: it is based on a combination of Extended Kalman Filtering, with series of geometrical transformations applied for drift correction during certain mask periods, under a certain condition.

As concerns the Extended Kalman Filter, a comprehensive set of odometric models of vehicles is described, considering for instance that the encoder can be located at front or rear wheels.

INTRODUCTION

The interest in techniques of localisation of vehicles is growing, not only for professional applications like road maintenance or fleet management, but also for all future applications which address personal vehicles automatic control.

This paper addresses the localisation of survey vehicles for road maintenance. Geo-synchronous satellites services provide differential GPS corrections suitable for this kind of application. Nevertheless, the measurements collected by these vehicles need to be localised with a one meter precision for regional itineraries, including urban environments. As it is not necessary that this localisation process occurs in real time, smoothing techniques can be applied afterwards to the sensors measurements stored by an acquisition unit. As they operate in a context where "non causal" processing can be done, the data can be filtered in both forward and backward direction, and finally combined.

On another hand, DGPS masks do not allow a continuous localisation and therefore dead-reckoning sensors are necessary to estimate the position of the vehicle during these situations.

In [Bétaille and Bonnifait, 00], we have presented an algorithm for post-processing the trajectory of the vehicle which is based on a Bayesian fusion of the estimations of Extended Kalman Filters corrected by series of geometrical transformations (which is the main originality of our solution) applied for drift correction during mask periods.

The works reported in the present paper aimed at:

- improving the result of preceding tests relatively to the model of the vehicle, considering for instance that the encoder can be located at front or rear wheels;

- proposing a solution to a drawback of the use of similarities in certain masked areas.

It is important to stress that the improvement that we seek to obtain in the vehicle modelling is also applicable in real-time operation, and not only in post-processing.

In section 1, the sensors on board the vehicle are presented. Section 2 is dedicated to the presentation of different odometric models. Section 3 is devoted to a study in simulation, which enables a detailed analysis of the models to be carried out. In section 4, experimental tests performed with real data quantifies the performances of the different solutions. The model we suggest to use is then tested in full scale in section 5 in a filtering process with real data. A particular attention is given to the sampling frequency which plays an important part on the quality of the result. Finally, section 6 highlights a problem in using the similarities for the smoothing process during certain mask periods. We show the effectiveness of a heuristic strategy that consists to not apply the similarities in certain situations.

1. The localisation sensors on board.

1.1. GPS.

Differential GPS appears naturally very appropriate to provide the geographical coordinates of survey vehicles, for further use in a Geographical Information System (GIS) [Abbott and Powell, 99].

The precision of one meter over wide areas (several hundreds of kilometers may be performed in the frame of our applications) can be achieved in differential GPS with dedicated services, provided in Europe by geo-synchronous satellites like "Landstar" or "Omnistar", with no significant degradation of the precision or frequent problem of reliability.

The receiver on board the vehicle was a TRIMBLE Ag132 (GPS code on L1 frequency) running in DGPS, at 5 Hz, by using one of the differential correction services available in Europe. The standard deviation of the positioning error obtained during recent static tests of this equipment was 0.5 m, with no SA.

Note that the differential corrections may be biased (they are actually in the region of Nantes, west of France, by approximately 0.7 m), which therefore gives a global "geodetic" offset when downloading the vehicle trajectory into GIS with reference mapping of 1 meter accuracy.

Unfortunately, DGPS cannot offer a continuous positioning. Masks of the satellites will cut off the signal, particularly in difficult environments like cities or forests. Furthermore, to avoid diffraction or multipath contamination of the positioning results, raw data should be carefully filtered, by setting-up relatively high elevation mask (20°) and low DOP level. It is actually preferable to cope with larger masks than to input aberrant positioning in the data filtering and smoothing process.

Dead-reckoning sensors are obviously needed in this process, in order to help DGPS in case of masks occurrences. They are two of them on board our vehicle:

- an electro-mechanical shaft type encoder
- a fiber-optic 1 axis (heading) gyrometer

1.2. Encoder.

Our vehicle is doted of an encoder, which has been calibrated using a Post-Processed Kinematic (PPK) GPS, in static mode, between two stations (situated on a straight line of length 1000 m) at which the vehicle stopped. We estimate that the uncertainty of the calibration equals 1 "step" of the encoder per the performed distance, supposing that:

- the wheels do not slip,
- the rolling surface is perfectly planar,
- the PPK GPS location produces a negligible error.

The estimated length of the step of the encoder is 0.24 m, with an error of less than 1%.

Note the step could be one of the estimated variables, like position and heading, in the process shown below. With the set of sensors installed on board our vehicle, it is easy to prove the observability of the length of the encoder step, additionally to the position and heading, with the only condition of an effective movement of the vehicle (non static) [Bonnifait, 97]. A balance is to be found in the tradeoff between reliability (ability to identify a rather improbable variation of the length of the encoder step, for instance) and robustness. This particular point should be addressed in our further studies.

1.3. Gyrometer.

The vehicle is equipped by a "KVH" fiber optic gyrometer (RD 2100 digital model), which works by application of the "Sagnac effect" principle. It outputs the heading rotation speed at the frequency of 10 Hz. Since the rotation speed is measured, the heading is obtained by integration in the process after.

The characteristic of the drift of the KVH RD 2100 gyrometer is around 10 degrees per hour.

Furthermore, a Fourier analysis of the signal output during dynamic tests (in the real condition of use with our vehicle) enabled the level of noise to be set up, and an acceptable value is 0.1°/s.

1.4. Data collecting.

The following measurements:

- 5 Hz GGA positioning output of the Ag132,
- 10 Hz digital output of the gyrometer,
- GPS "pulse per second" output,

were collected on a PC by interrupts, and dated using a PC clock whose resolution was 0.01 s. The encoder steps counter is also read at 10 Hz (at each output of the gyrometer). The GPS pulse per second (delivered by a TRIMBLE 7400 receiver on board, see § 4) was used to synchronize the GPS time and the PC clock in the data fusion post-processing.

2. Integration of the odometer and gyrometer data in “rear” and “front” odometric models.

2.1. Rear odometric model.

The usual odometric model of a vehicle follows the following discrete equations [Bonnifait and Garcia, 98], where "x" and "y" are the coordinates of the middle of the rear wheels of the vehicle (point M, see figure 1), in a local reference frame, and "θ" its heading:

$$x_{k+1} = x_k + \Delta s_k.\cos(\theta_k + \Delta\theta_k/2)$$

$$y_{k+1} = y_k + \Delta s_k.\sin(\theta_k + \Delta\theta_k/2) \quad (1)$$

$$\theta_{k+1} = \theta_k + \Delta\theta_k$$

"Δs" represents the variation of distance (measured at rear wheels) between two sampling instants and "Δθ" corresponds to the elementary variation of the heading. With a gyrometer, which gives a rotation speed, $\Delta\theta=\omega.Ts$, where "Ts" represents the sample time and "ω" the measured heading rotation speed.

Ideally, the model described in (1) applies to the origin of a mobile frame attached to the middle of the rear wheels of the vehicle, with a measurement by the encoder of the average rotation of these wheels, and with the front wheels for steering. Mathematically, these wheels are equivalent to a unique virtual front steering wheel, whose axis, like the one of the actual wheels, crosses the instantaneous center of rotation of the vehicle.

We suppose that:

- the distance measured by the encoder is the one of the origin of the mobile frame (wheels do not slip),
- the trajectory is locally circular.

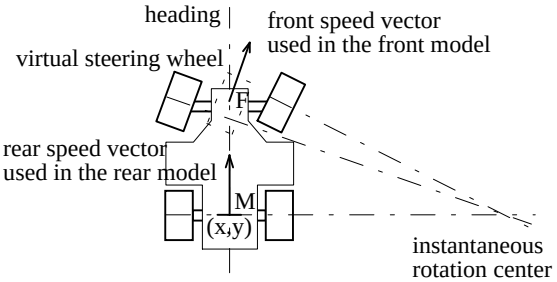

Fig.1: scheme of the vehicle (Ackermann model)

Actually, most vehicles are equipped of an encoder installed on the gearbox, and with front wheels for both steering and driving. Our testing vehicle is a Peugeot J5 minivan, and the encoder on this van measures effectively the rotation of the gearbox, which is the mean of the rotation of the front wheels on this vehicle. Moreover, the front wheels are the steering wheels.

Hence, the characteristics of our vehicle and its encoder location do not meet the requirement for applying the odometric model presented in (1).

2.2. Front odometric model.

If the encoder measures directly the rotation of the gearbox on a vehicle with front wheels for both driving and steering, then the odometric model is to be applied to the origin of a mobile frame attached to the middle of the front wheels.

Let consider point F (see figure 2), the middle of the front wheels of the vehicle and "xf" and "yf" its coordinates, in a local reference frame. We propose to derive an odometric model having the following equations:

$$xf_{k+1} = xf_k + \Delta sf_k.\cos(\theta_k + \beta_k)$$

$$yf_{k+1} = yf_k + \Delta sf_k.\sin(\theta_k + \beta_k) \quad (2)$$

$$\theta_{k+1} = \theta_k + \Delta\theta_k$$

with β_k to be determined.

"Δsf" represents the variation of distance (measured at front wheels) between two sampling instants and "Δθ" still corresponds to the elementary variation of the heading.

The next figure enables equations (2) to be completed.

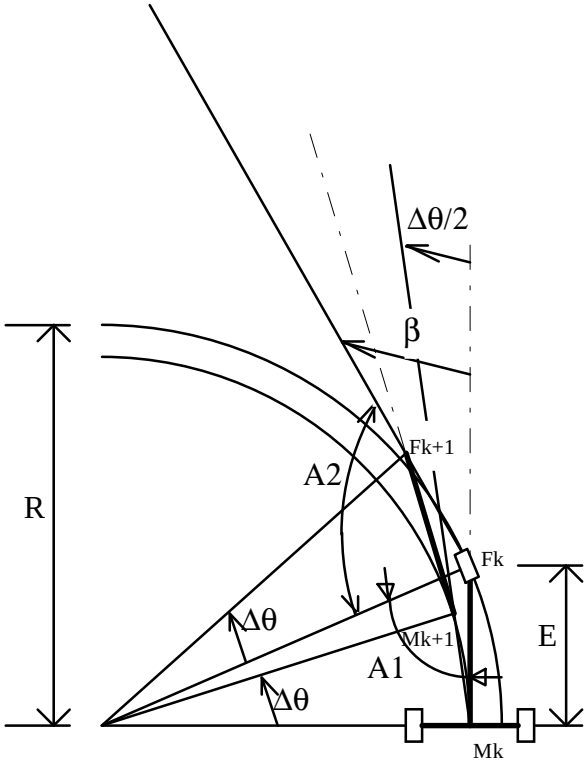

Fig.2: front odometric model

Geometrically, it appears that:

$$\beta = \pi - A1 - A2 \quad (3)$$

with:

$$A1 = \arccos(E/R_k) = \arccos(E.\Delta\theta_k/\Delta sf_k)$$

$$A2 = (\pi - \Delta\theta_k)/2$$

So: $\beta = \Delta\theta_k/2 + \arcsin(E.\Delta\theta_k/\Delta sf_k)$

Note $\Delta sf_k/\Delta\theta_k$ is an estimation of the radius of curvature, R_k. For large curves, $E<<R_k$. E is the distance between M and F, or wheelbase.

Consequently, by using the development of Taylor of the arcsin:

$\beta_k \sim E.\Delta\theta_k/\Delta sf_k + \Delta\theta_k/2$ (4)

In a straight line, the only term remaining is $\Delta\theta_k/2$, which corresponds to equations (1).

The front model is equal – at the first order – to other models identified in the literature [Bonnifait et al., 01], [Kochem et al., 02]). It appears to be theoretically an adequate odometric model to be applied onto our testing vehicle.

2.3. Odometric model for any point of the vehicle.

The equations in (1) or (2) describe the evolution of the origin of a mobile frame (M or F), attached to the vehicle, with a specific location in the vehicle: the middle of rear wheels, or the middle of front wheels. It may be of great interest to derive the similar equations for any other point of the vehicle, particularly when combining these equations with positioning estimation by DGPS. Then, we will not presume of the actual position of the DGPS antenna relatively to the vehicle, and we will introduce the translation parameters "tx" and "ty" of the antenna relatively the mobile frame used in the model.

$$xf_{k+1} = xf_k + \Delta sf_k.\cos(\theta_k + \beta_k) + \Delta\theta_k.(t_X.\sin\theta_k + t_Y.\cos\theta_k)$$

$$yf_{k+1} = yf_k + \Delta sf_k.\sin(\theta_k + \beta_k) + \Delta\theta_k.(t_X.\cos\theta_k - t_Y.\sin\theta_k) \quad (5)$$

$$\theta_{k+1} = \theta_k + \Delta\theta_k$$

3. Performances of "rear" and "front" models in simulation.

3.1. Set up reference points series.

We are going to demonstrate in simulation the interest of the front model.

Suppose the vehicle is performing a perfect circle with a radius of R=100 m (for illustrating purpose, note R=5 m on figures in xy plane). Heading steps are supposed to be constant, named "Δθ". The number of steps equals :

$n = 2\pi/\Delta\theta$ (6)

As well as angle steps, distance steps are supposed to be constant, named "Δs" (for rear point) and "Δsf" (for front point).

Let us name "rear point" the middle of the rear wheels (represented by point M on figure 1), and "front point" the middle of the front wheels (point F on figure 2).

For the rear point: $\Delta s = R.\Delta\theta$

For the front point: $\Delta sf = \sqrt{R^2+E^2}.\Delta\theta$

where E is the distance between M and F. E=5 m for numerical application purpose (for illustrating purpose again, E=2 m on figures in xy plane).

The reference position of the rear point is given by the points series:

$M_k(X_k,Y_k)$

$X_k = R.\cos(k.\Delta\theta)$

$Y_k = R.\sin(k.\Delta\theta)$

for k=1 to n.

The reference position of the front point is given by the points series:

$Fk(Xf_k,Yf_k)$

$Xf_k = \sqrt{R^2+E^2}.\cos(k.\Delta\theta + \text{atan}(E/R))$

$Yf_k = \sqrt{R^2+E^2}.\sin(k.\Delta\theta + \text{atan}(E/R))$

for k=1 to n

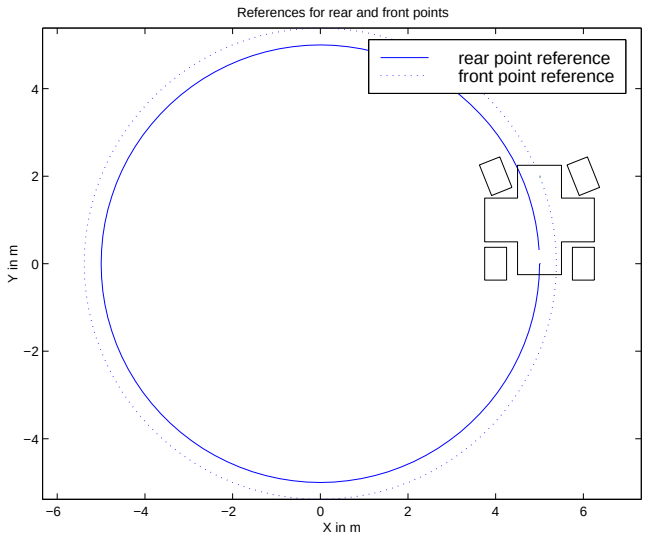

Fig.3: reference points series

3.2. Different uses of the rear model.

Let us suppose that we have an encoder measuring the performed distance of the rear point.

3.2.1. Nominal use.

Firstly, we are going to compute the position of the rear point, by using the rear model applied onto the rear point. Δs (distance performed by the rear point) and Δθ are input.

Initial rear point coordinates are x=R, y=0, $\theta=\pi/2$.

The following figure displays the difference between x and y series output by the model, and the corresponding reference series. The error is due to the fact that Δs is applied on the chord instead of the arc. It decreases with Δθ (i.e. when the frequency of the gyrometer increases). It can be demonstrated that the maximum value of error "Emax" equals:

$Emax = 2R.((\pi/n)/\sin(\pi/n)-1) \sim R.(\pi/n)^2/3$ (7)

with "n" given in equation (6).

Table 1 gives a numerical application for different values of n.

table 1

n	100	200	400
Δθ	2π/100	2π/200	2π/400
Error	0.03	0.01	0.002

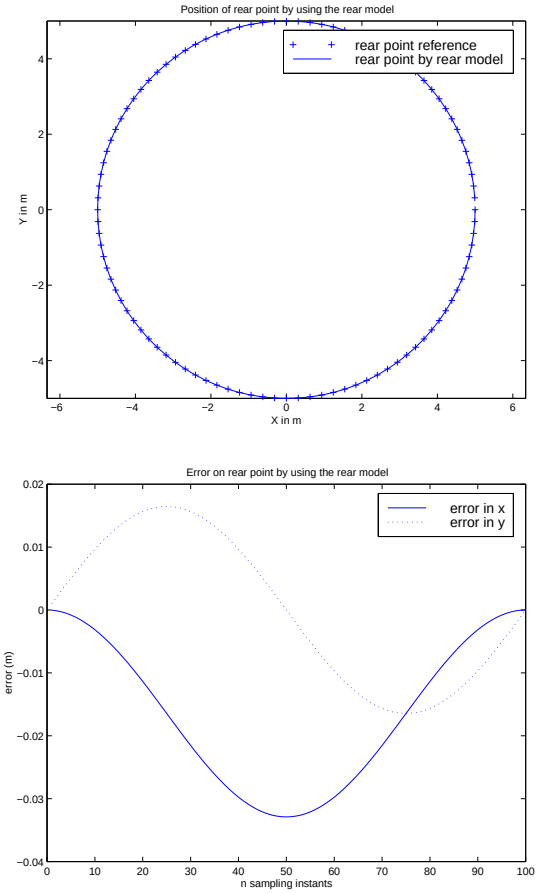

Fig.4: positioning rear point with rear model

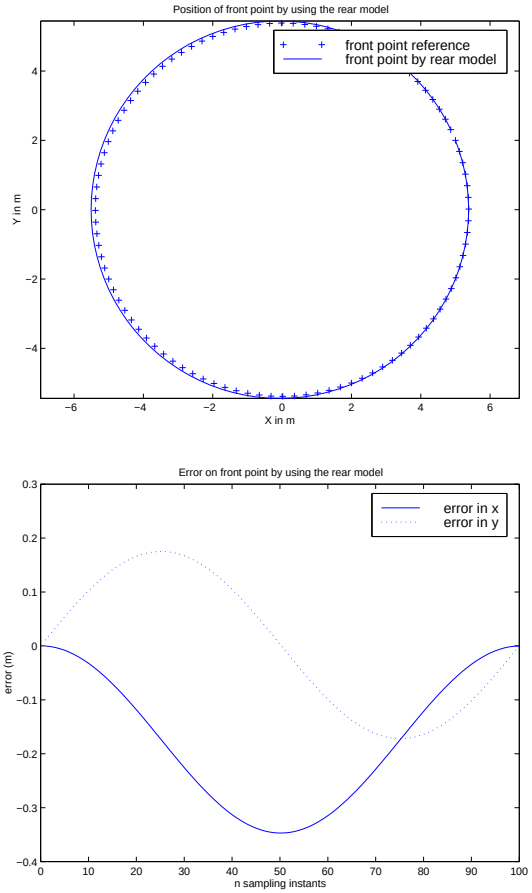

Fig.5: positioning front point with rear model

3.2.2. Positioning error on front point.

Next, let us compute the position of the front point, by using the rear model applied onto the rear point, and the translation terms from rear point to front point: tx=E and ty=0. Δs (distance performed by the rear point) and Δθ are input.

Initial front point coordinates are x_f=R, y_f=E, θ=π/2.

The following figure displays the difference between x_f and y_f series output by the model, and the corresponding reference series. The error is due to the fact that cos(Δθ)~1 and sin(Δθ)~Δθ in derivating the model available for any point of the vehicle, given in equations (5). This error decreases with Δθ,i.e. when the frequency of the gyrometer increases (see table 2).

table 2

n	100	200	400
Δθ	2π/100	2π/200	2π/400
Error	0.3	0.15	0.08

Let us now suppose that we have an encoder measuring the performed distance of the front point.

The problem is to compute the position of the rear point. The rear model may be used in two different ways.

3.2.3. Use of the rear model with the distance performed by the front point.

Firstly, we are going to compute the position of the rear point, with the assumption that the rear and front points both perform the same distance, by using the rear model applied onto the rear point. Δsf (distance performed by the front point) and Δθ are input.

Initial rear point coordinates are x=0, y=R, θ=π/2.

The following figure displays the difference between x and y series output in this first case, and the corresponding reference series. The maximum value of the error equals:

$$Emax = 2R.(\sqrt{(1+E^2/R^2)}-1) \qquad (8)$$

It equals 0.25 m in our example.

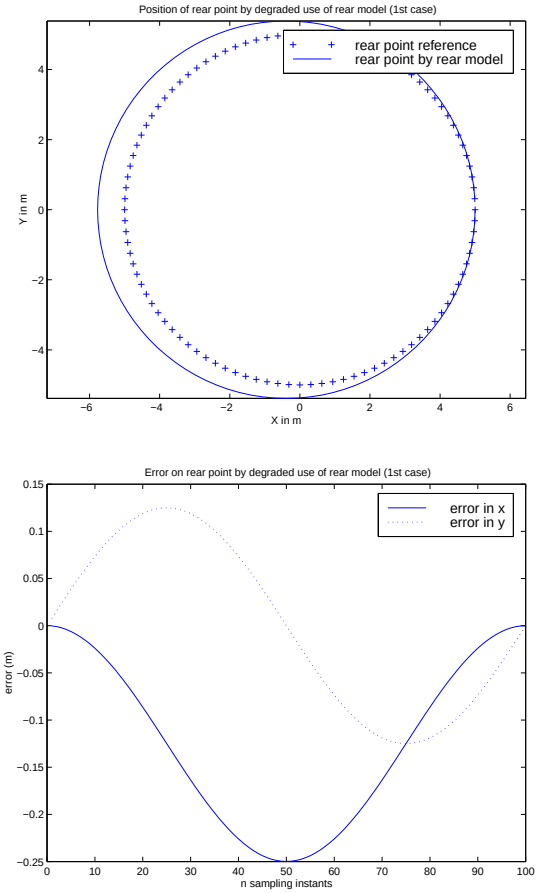

Fig.6: use of the rear model with the distance traveled by the front point

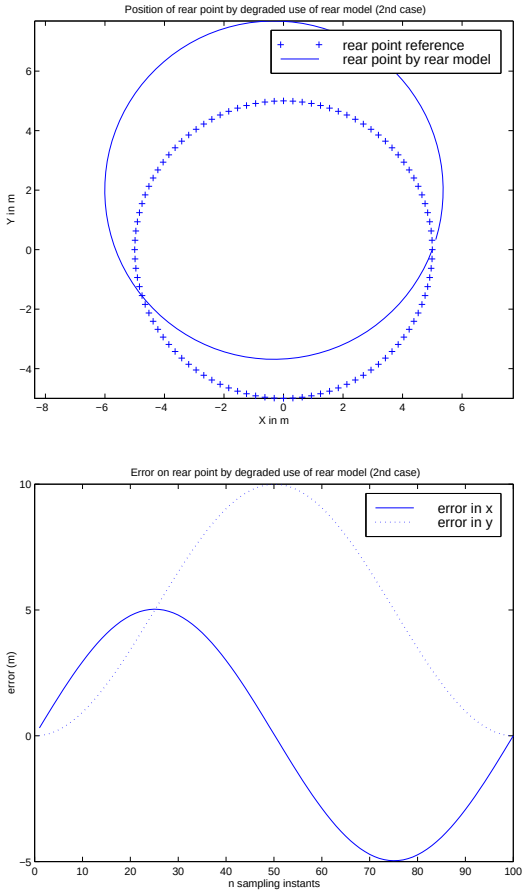

Fig.7: use of the rear model applied onto the front point

Note that the error does not depend on Δθ (frequency of the gyrometer) because the arc-chord approximation (see equation (8)) is negligible with respect to the modeling error.

3.2.4. Use of the rear model applied onto the front point.

Secondly, we are going to compute the position of the rear point, by using the rear model applied onto the front point, and the translation terms from front point to rear point: tx=-E and ty=0. Δsf (distance performed by the front point) and Δθ are input.

Initial rear point coordinates are x=0, y=R, θ=π/2.

The following figure displays the difference between x and y series output in this second case, and the corresponding reference series. The maximum value of the error equals:

Emax = 2E (9)

It equals 10 m in our example.

For the same reason as already mentioned in § 3.2.3, the error does not depend on Δθ (frequency of the gyrometer).

Conclusion.

Firstly, the nominal use of the rear model is obviously the best to do, even when measuring the performed distance of the front point.

Secondly, if the evolution of the front wheels is needed, it is better to use the nominal model and make the translation tx and ty, instead of measuring the distance on the front wheels.

3.3. Use of the front model.

The front model is specifically designed to fit with the evolution of the front point.

We are going to compute the position of the front point, by using the front model applied onto the front point. Δsf (distance performed by the front point) and Δθ are input.

Initial front point coordinates are x_f=R, y_f=E, θ=π/2.

The following figure displays the difference between x_f and y_f series output by the front model (with no development of the arcsin included in the model, and also with this development), and the corresponding reference series. The error is again due to the approximation of the arc by the chord. An additional error (depending on the ratio E/R) comes from the development of the arcsin when this is done.

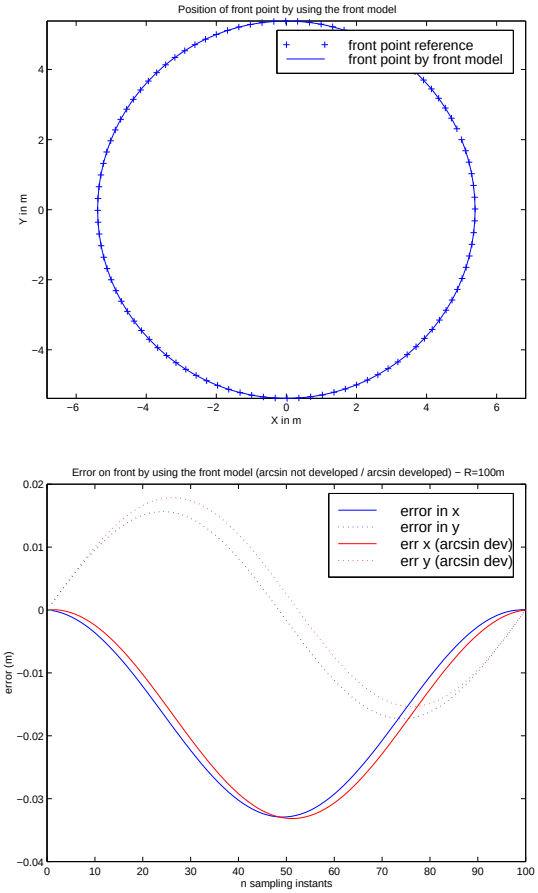

Fig.8: use of front model for front point positioning E = 5 m and R = 100 m

When the arcsin is not developed, it can be demonstrated again that the maximum value of error "Emax" equals: Emax ~ sqrt(R^2+E^2).$(\pi/n)^2/3$.

It is the same as Emax reported in equation (7) but with sqrt(R^2+E^2) instead of R.

Note: the maximum value of the error, if the arcsin is developed (Taylor's series), has been obtained in simulation.

Note that the errors – with and with no development of Taylor – are about the same with E=5 m and R= 100 m, but get very different with E=2 m and R= 5 m.

table 3

n	100	200	400
Δθ	2π/100	2π/200	2π/400
Error (R=100 m E=5 m)	0.03	0.01	0.002
	0.03 if arcsin is developed, indep. of n		
Error (R=5 m E=2 m)	0.002	0.0005	0.0001
	0.1 if arcsin is developed, indep. of n		

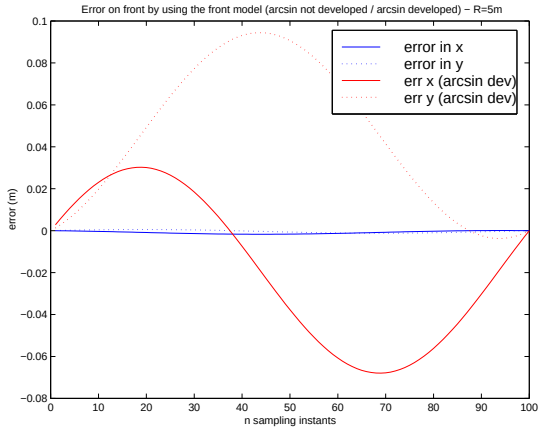

Fig.9: use of front model for front point positioning E=2 m and R = 5 m

So, if the evolution of the front wheels is needed, it is the best to use the front model and the distance performed by the front wheels.

This simulation shows that by using an adequate model onto front point (front wheels), we can reduce the error that we would obtain in case of misusing the rear model.

4. Comparison of the models with real data.

We have seen in simulation that two different degraded use of the rear model may give an approximation of the trajectory of the vehicle.

The first approximation consists in applying equations (1) to the mobile frame attached to the middle of the rear wheels with the measurement Δsf of the rotation of the front wheels (instead of that of the rear wheels).

The second approximation consists in applying equations (1) to the mobile frame attached to the middle of the front wheels with Δsf too.

The simulation definitely proved that the last one is causing much more error than the first one. The model corresponding to equations (1) is indeed valid exclusively for the non steering wheels whereas the front wheels are actually the steering ones with our vehicle.

Consequently, only the first approximation (use of the rear model with the distance performed by the front point) and the front model itself are going to be tested in parallel, with exactly the same data.

The tests reported in this section were performed at low speed (10 km/h maximum) on the LCPC tracks, near Nantes. The steering wheels of the minivan were turned to their maximum angle, firstly on the right hand side and secondly on the left hand side.

A centimeter precision reference path was computed for each test, by RTK GPS at 5 Hz. Two TRIMBLE 7400 receivers (GPS L1 and L2 carrier) were used, one antenna on a monument in the vicinity of the circuit, the other on top of the roof of the minivan (see figure 10). The environment of the circuit offers excellent conditions to perform GPS measurements, with no natural masks (the reference was thus obtained continuously).

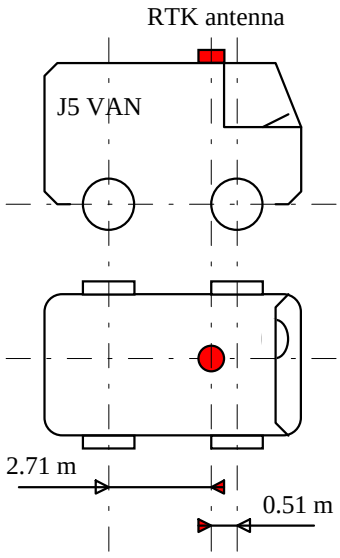

Fig.10: the equipped minivan scheme (RTK antenna)

The trajectory was firstly computed by using the rear model. The rear model describes the odometry of the rear point. Whereas the distance is measured on the front wheels, it is applied onto the rear model. Translation parameters are also used (see § 2.3), from rear point to reference point: tx=2.71 m and ty=0.

The trajectory was secondly computed by using the front model. The front model describes the odometry of the front point, where we effectively have the distance measured. Again, translation parameters are used from front point to reference point: tx=-0.51 m and ty=0.

Note that the trajectory computed here is only obtained by integrating distance and rotation measurements (odometer and gyrometer) and it does not use GPS for filtering or smoothing purpose (GPS only provides a reference here).

From visual inspection, it clearly appears that the front model gives a better estimation of the position of the reference point than the rear model.

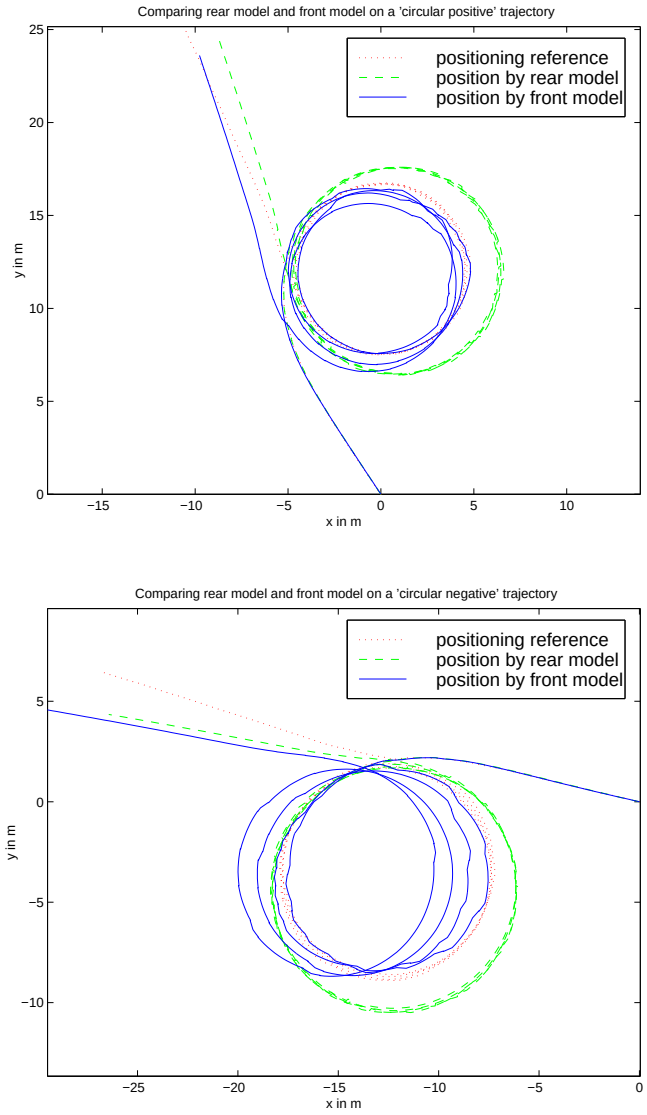

Fig.11: comparison of rear and front models on circular trajectories.

An immediate conclusion is that when the radius of curvature is small, it is better to use the front model than to misuse the rear model.

It is also worth to note that the front model seeks to estimate the radius of curvature ($\Delta\theta_k/\Delta sf_k$). It shows a level of noise relatively high when data are collected at 10 Hz compared to that shown if data were collected at 2 Hz for instance (at low speed, only 0, 1 or 2 steps are made in 1 sample). A decimation from 10 Hz down to 2 Hz gives better results (illustrated in figure 12). Another solution would be to use an encoder with a lower step value in order to refine the measurement of distance.

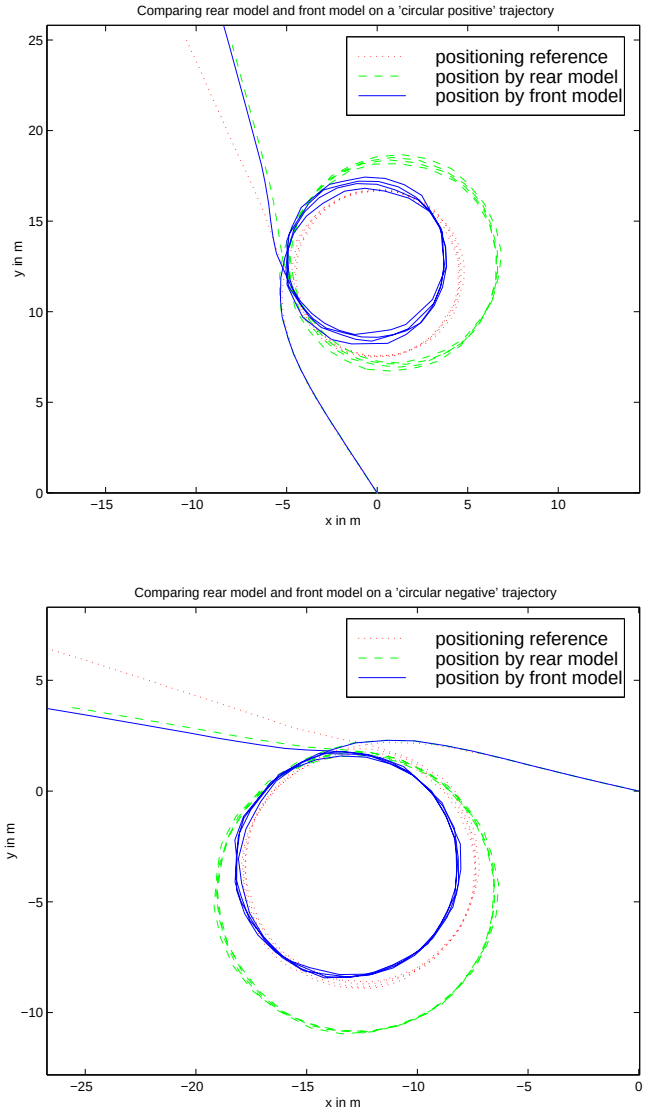

Fig.12: comparison of rear and front models on circular trajectories,
with data decimated from 10 down to 2 Hz.

From visual inspection again, it appears that a good estimation of the radius of curvature is possible at 2 Hz, since the distance performed in a sample time is sufficient, and the obtained trajectory is less noisy than at 10 Hz.

5. Fusion of odometry and DGPS data.

The tests reported in this section were performed at three different average speeds (20, 40 and 60 km/h) on a circuit near Nantes. The maximum speed not to exceed was 90 km/h. Again, a centimeter precision reference path was computed for each test, by RTK GPS. No natural masks around the circuit perturbed the GPS or DGPS reception. (DGPS masks were in fact simulated for this study).

The DGPS antenna is represented on the next figure, close-by the RTK reference antenna.

Only the first approximation (use of the rear model with the distance performed by the front point) and the front model itself are going to be tested in parallel, both with data collected during the tests on circuit.

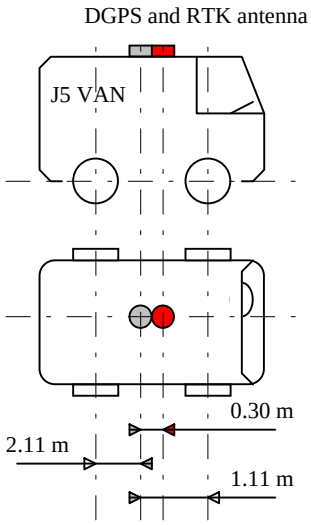

Fig.13: the equipped minivan scheme
(DGPS and RTK antennas)

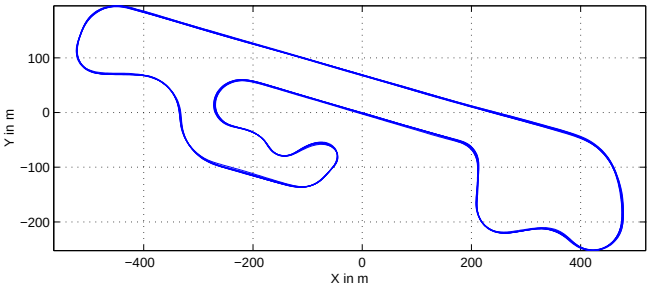

Fig.14: experimental circuit

The point which needs an evolution model is the DGPS antenna (see figure 13), in order to facilitate the formulation of the Extended Kalman Filter. Hence, ty = 0 (the antenna is centered); but:

tx = 2.11 m (in front of the rear wheels axis), in case of the degraded use of the rear model;

tx = -1.11 m (behind the front wheels axis), in case of use of the front model.

The derivation of the equations used in the filter can be found in [Bétaille and Bonnifait, 00]. It gives the formalism of an Extended Kalman Filter (EKF) to fuse the encoder and gyrometer data, and the DGPS locations. Note that contrary to the hypothesis made in that paper (where we supposed that the DGPS antenna was located on the vertical axis of the mobile frame), the model and Jacobian matrixes to be computed are slightly more complicated, because of the translation terms tx and ty.

The variances of both the DGPS receiver and the gyrometer measurements were estimated a priori, and based upon static tests (for the DGPS receiver: $(0.5\ \text{m})^2$) and dynamic tests (for the gyrometer: $(0.1°/\text{s})^2$).

Besides, the variance of the measurements of the distance equals: $\text{step}^2/12$.

The variances for the model were tuned so that the error between the filtered path and the reference path is always comprised into a 3σ envelope, where σ are obtained for both x and y coordinates (diagonal elements of the variance EKF output matrices).

The filter was tuned on the registered data for the test at lower speed (for which wheels slipping is reduced). We simulated the obscured periods by suppressing the DGPS data for a series of masks of 60 s, separated by 10 s periods of available DGPS locations.

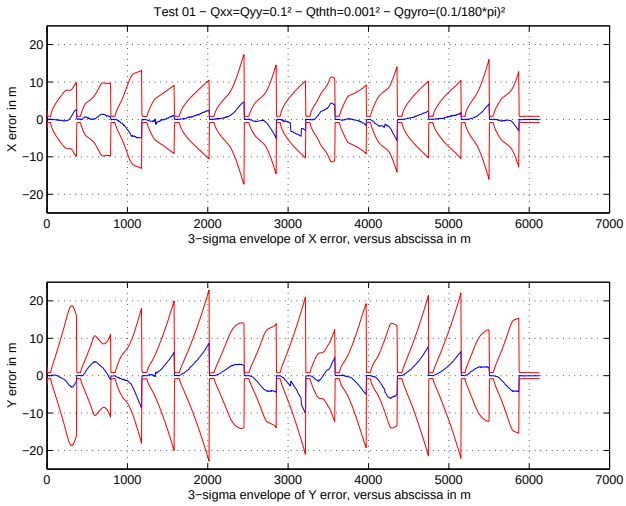

Fig.15: positioning errors and 3σ envelopes

table 4

Test nb	Rear model	Front model
1 (20 km/h)		
Error maxi	14.6 m	10.6 m
RMS	3.7 m	3.3 m
2 (40 km/h)		
Error maxi	17.6	17.1
RMS	6.1	3.6
3 (60 km/h)		
Error maxi	19.5	25.5
RMS	4.3	6.0

Note: the error is computed between the filtering process output x and y coordinates, and the x and y references, at same time, given by RTK GPS.

It appears that the interest of using the front model in the fusion with DGPS decreases when the speed gets high.

We have to keep in mind that the position prediction during a DGPS mask shows a drift which is explained by:

- the drift of the gyro itself,
- the approximation of the non-linear integration model,
- the fact that the road is not perfectly planar,
- the slipping of the wheels.

The behaviour of the filter when using the front model shows a certain instability. This may be due to:

- the additional error term corresponding to β_k;
- the high sensitivity of the front model with slipping, since slipping biases the estimation of the radius of curvature;
- the additional non-linearity in the Kalman filter.

Considering these results, it is clear that the filtering must be completed with smoothing, if non-causal data processing is possible.

6. The geometrical smoother by similarities and a condition of use.

[Bétaille and Bonnifait, 00] compared several non-causal filters which can be directly computed from EKF outputs because they use the same formalism.

We had observed that the main drawback of the EKF is that the heading estimation is less corrected than the position, in the estimation step of the filter, when a DGPS measurement is available after a GPS mask. We had noticed that a simple similarity applied on the positions between two DGPS estimations significantly improve the precision, even when these estimations are separated by some tenths of seconds due to GPS masks.

The parameters (rotation and scale factor) are calculated in order to superpose the final predicted position with the new estimated DGPS position. This transformation repeats each time a DGPS estimation is used to correct a series of dead-reckoning predictions.

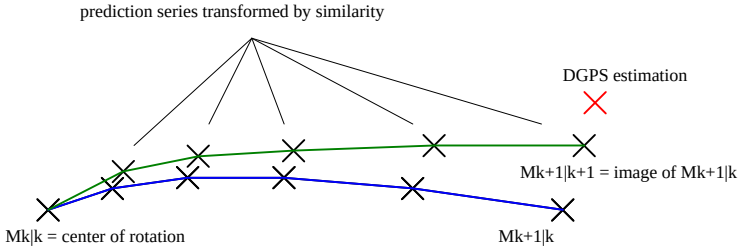

Fig.16: graphical illustration of the similarity

The next figure illustrates a critical use of the similarity and the necessity of setting a condition before deciding to apply such a geometric transformation.

In this figure, the geometrical elements Mk|k, Mk+1|k and Mk+1|k+1 used to compute the similarity have a configuration that causes a very large correction to be made in part of the trajectory.

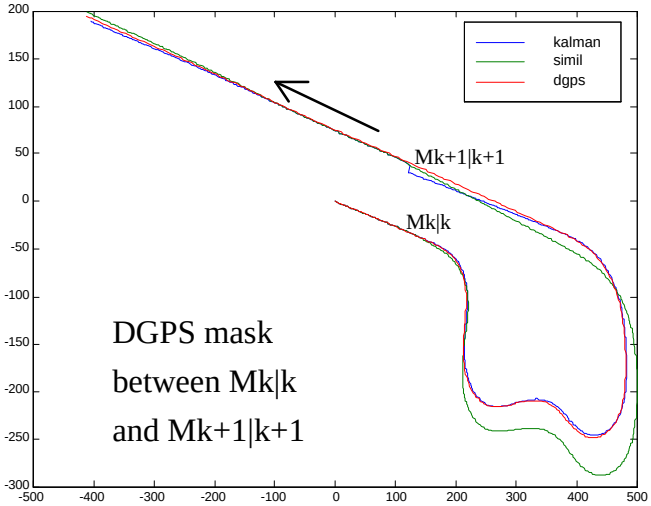

Fig.17: critical use of the similarity

A simple way to circumvent the problem is to check if the trajectory is contained in a band twice wide the distance between the two DGPS estimated points (Mk|k and Mk+1|k+1) used in the definition of the similarities.

The next figure illustrates the condition applied onto similarities.

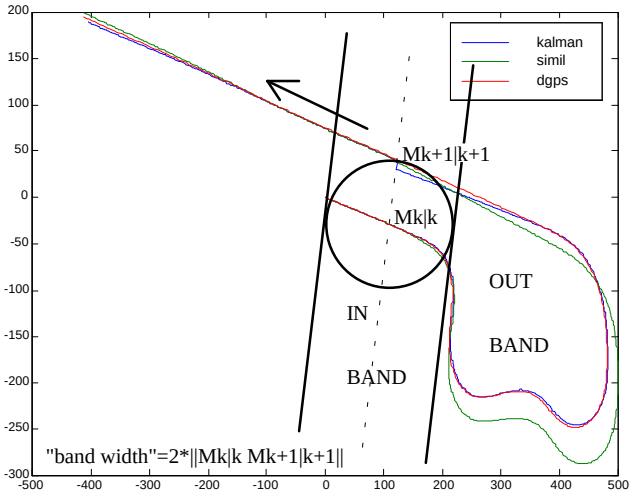

Fig.18: graphical illustration of the conditional similarity

Between the two DGPS estimated points: Mk|k and Mk+1|k+1, the trajectory is NOT contained in a band twice wide the distance || Mk|k Mk+1|k+1 ||. No similarity is applied. On the contrary, it is applied further on the circuit, and each time where the trajectory does not show circumvolutions.

The complete algorithm uses the front model and runs by the following steps:

- compute forward trajectory, and store the full variance-covariance matrices associated to the x and y positions,
- apply the conditional similarities, and compute "modified" variance-covariance matrices (the similarities are actually non determinist and they modify the stochastic properties of x and y),
- compute backward trajectory, and do the same treatment with x and y positions and their variance-covariance matrices,
- combine in a Bayesian fusion x and y obtained forward and backward by the preceding treatments; "modified" variance-covariance matrices are to be used in the fusion.

table 5

Test nb	filtering real-time process	smoothing post-process (*)
1 (20 km/h)		
Error maxi	10.6 m	3.4 m (3.4 m)
RMS	3.3 m	0.9 m (1.0 m)
2 (40 km/h)		
Error maxi	17.1	3.4 (5.8)
RMS	3.6	1.2 (1.7)
3 (60 km/h)		
Error maxi	25.5	6.0 (9.1)
RMS	6.0	2.0 (2.7)

(*): into () in table 5 are reported statictics if no condition of use of the similarities is applied.

As expected, this combination of the smoothed trajectories gives the best results and approaches the level of precision required by the application. It also could be noticed that (contrary to real-time filtering process) smoothing post-process results are quite similar irrespective of using the rear or front model.

CONCLUSION

With these new experimental results, we can discuss the interest of refining the modelisation of the vehicle. The model presented in the paper is more accurate than that used in general case, but it is also more sensitive to noise in measurements. Therefore, the global performance of the smoother is not improved. An adequate acquisition and filtering process is worth to be studied further, in particular in order to obtain a good estimation of the radius of curvature.

Lastly, the test condition of the similarity carries out real improvements to the smoothing technique that we presented in ION 2000. It makes us tackle the objective of localising a vehicle at 1 m precision, using a low-cost gyrometer, an odometer and DGPS, despite a series of masks considered to be particularly severe.

ACKNOWLEDGEMENTS

Thanks to Charles Lemaire for its technical assistance.

REFERENCES

[Abbott and Powell, 99]: E. Abbott and D. Powell. "Land-Vehicle Navigation using GPS". Proceeding of the IEEE, Vol. 87, NO. 1, January 1999.

[Bétaille and Bonnifait, 00]: D. Bétaille and Ph. Bonnifait. "Road Maintenance Vehicles Location using DGPS, Map-Matching and Dead-Reckoning: Experimental Results of a Smoothed EKF". IAIN & ION 2000, June 2000, pp. 328-342.

[Bonnifait, 97]: Ph. Bonnifait. Phd Thesis. Université de Nantes.

[Bonnifait and Garcia, 98]: Ph. Bonnifait and G. Garcia. "Design and Experimental Validation of an Odometric and Goniometric Localisation System for Outdoor Robot Vehicles". IEEE Transactions on Robotics and Automation. Vol. 14, NO. 4, August 1998, pp. 541 - 548.

[Bonnifait et al., 01]: Ph. Bonnifait, P. Bouron, P. Crubillé, D. Meizel. "Data Fusion of Four ABS Sensors and GPS for an Enhanced Localization of Car-like Vehicles". IEEE International Conference on Robotics and Automation (ICRA 01), Seoul, May 2001, pp. 1597-1602.

[Kochem et al., 02]: M. Kochem, N. Wagner, C.-D. Hamann, R. Isermann. "Data Fusion for Precise Dead-Reckoning of Passenger Cars", 15th Triennal World Congress IFAC 02, Barcelona, July 2002.